Boosting Oxidase-Mimicking Activity of Metal-Organic Framework Nanozymes via Heteroatom Modulation in Organic Linkers

Yan Wei, ‡[a] Qiming Yan,‡[b] Zizhe Yan, [a] Jinle Yang, [a] Liuhan Zhang, [a] Feng Li*[a], Dangqiang Zhu*[a, c]

[a]College of Chemistry and Pharmaceutical Sciences, Qingdao Agricultural University, Qingdao 266109, People's Republic of China

[b]School of Chemistry and Chemical Engineering, Liaocheng University, Liaocheng 252000, People's Republic of China

[c]Key Laboratory of Flexible Optoelectronic Chemical Materials and Devices, Ministry of Education, Jianghan University, Wuhan 430056, People's Republic of China

∗ *E-mail address*: zhudq@qau.edu.cn (D. Zhu); lifeng@qau.edu.cn (F. Li)

Experimental section

Regents and Materials: Iron trichloride hexahydrate ($FeCl_3 \cdot 6H_2O$), 1,4-dicarboxybenzene (BDC), 2,5-furandicarboxylic acid (FDC), 2,5-thiophenedicarboxylic acid (TDC), 2-nitro-1,4-benzenedicarboxylic acid (BDC- NO_2), 3,3',5,5'-tetramethylbenzidine dihydrochloride (TMB) and N,N-Dimethylacetamide (DMA) were obtained from Macklin Biochemical Co. Ltd. (Shanghai, China). thiocyanate (KSCN) and Ethylenediaminetetraacetic acid disodium salt (EDTA), was purchased from Aladdin Co, Ltd. (China). All experimental water was obtained from the Milli-Q Water Purification System. All reagents are analytically pure and can be used without further purification.

Apparatus: The surface morphology of the MOF nanozymes were characterized by TEM HT7700 (Hitachi, Japan). XPS ESCALAB 250Xi (Thermo Fisher Scientific, USA), and XRD Bruker D8 Advance X-ray diffractometer (Bruker, Germany) were employed to study the composition and valence state. Raman spectrometer (Thermo Scientific) with an excitation wavelength of 532 nm. Zeta potential was tested on a Zetasizer Nano ZEN3690 (Malvern Instruments Ltd., Malvern, UK) to study the surface change of MOF nanomaterials under different conditions. UV-vis spectra were gotten from an UV-1800 spectrophotometer (Shimadzu, Japan) to evaluate the catalytic activity. The molecular frontier orbital energy levels and electrostatic potential surfaces were calculated by Gaussian software. CV characterizations were carried out on an Autolab electrochemical workstation (Metrohm, Netherlands) in the potential range from -0.2 to 0.8 V by using a three-electrode system: nanozyme modified ITO working electrode, Ag/AgCl reference electrode and platinum counter electrode with scanning rate was 100 mV/s.

Synthesis of MOF nanozymes: MIL-53(Fe)-L were synthesized by hydrothermal method. Organic linker (0.1 mmol), and $FeCl_3 \cdot 6H_2O$ (0.1 mmol) were dissolved in 12.0 mL DMA to obtain clear solution. Then, the mixture was transferred into a Teflon-lined stainless-steel autoclave for thermal treatment (150 ^oC, 3 h). After cooling down to room temperature, the solids were collected and washed with ethanol and water for

three times, which were further dried under vacuum at 60 °C for 12 h.

For MIL-88B(Fe)-L, organic linker (1.0 mmol), and $FeCl_3 \cdot 6H_2O$ (1.0 mmol) were mixed in 25 mL N.N-dimethylformamide. Then, 0.4 mL of NaOH solution (2 M) was added dropwise under vigorous stirring. The yellow solution was transferred into a Teflon-lined stainless-steel autoclave for thermal treatment (100 ^oC, 12 h). After cooling to room temperature, the solids were collected and washed with DMF, water and ethanol for three times, which were further dried under vacuum at 60 °C for 12 h.

Oxidase-like activity: 50 μL of nanozyme (200 μg/mL dispersion in water), and 50 μL of TMB (10.0 mM) were added to 400 μL of NaAc-HAc buffer (0.2 M, pH 4.0). After the incubation at 37 °C for 5 min, the UV–Vis spectra were monitored on a UV-1800 spectrophotometer. The effects of nanozyme/substrate concentration, pH and temperature various inorganic ions and amino acids (1 mM) on the OXD-like activity of MIL-53(Fe)-TDC were studied.

Catalytic kinetics assay: The kinetic assays were conducted by monitoring time-dependent absorbance change at 652 nm. Briefly, 20 μL of MOF nanozyme (0.2 mg/mL) and 20 μL of varying TMB concentrations (0.02-0.2 mM) were added into 160 μL of NaAc-HAc buffer (200 mM, pH 4.0). The catalytic system was incubated at 37 ^oC and the absorbance at 652 nm was recorded every 30 s for 3 min. The kinetic data was fitted to the typical *Michaelis−Menten* equation: $v = V_{max}[S]/(K_m + [S])$, where v is the initial velocity, [S] is the TMB concentration, K_m is the *Michaelis−Menten* constant, and V_{max} is the maximal reaction velocity.

Zeta potential measurement: Typically, 100 μL of 200 $\mu g \cdot mL^{-1}$ of nanozyme were added into 900 μL NaAc-HAc buffer (0.2 M, pH 4.0), and then the zeta potentials were measured. The time-dependent ζ potentials variation during the catalytic process were measured every 5 min for 30 min.

Detection of ROS by fluorescence assay: 2-(3,6-diacetoxy-2,7-dichloro-9H-xanthen-9-yl) benzoic acid (0.5 mg) was dissolved into 280 μL NaOH (10 mM) to obtain the DCF solution. After 30 min hydrolysis at 25 ^oC in the dark, the solution mixed with 1720 μL of PBS (25 mM, pH 7.4) to obtain DCF solution with a concentration of 0.25 mg mL^{-1}. 20 μL of MOF nanozyme (0.2 mg mL^{-1}) mixed with 20 μL of DCF solution.

Then the volume was adjusted to 200 μL by NaAc-HAc buffer (200 mM, pH 4.0). Following incubation at 37 ^{o}C for 30 min, the mixed solution was used for fluorescence measurements with an excitation wavelength of 488 nm.

Influence of various compounds on the catalytic activity: Briefly, 20 μL of MOF nanozyme (0.2 mg mL^{-1}) was mixed with 20 μL of interference compound (1.0 mM), and then 20 μL of TMB (10.0 mM) was added, which was further adjusted to 200 μL. After incubation at 37 ^{o}C for 5 min, the absorbance at 652 nm was monitored.

Electrochemical measurements: 2.0 mg MOF catalysts were dispersed in the mixture of H_2O (0.98 mL), and 5 wt% Nafion (20 μL) to form a homogeneous ink solution. Subsequently, 100 μL of the ink solution was dropped onto a ITO within a 0.5 cm × 0.5 cm coating area and then dried at room temperature. Cyclic voltametric measurements were carried out in 50 mM NaAc buffer solution (pH 4.0)

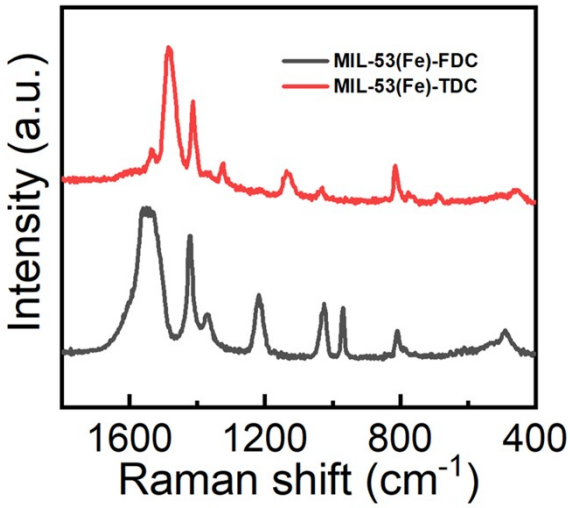

Fig. S1 Raman spectra of MIL-53(Fe)-FDC and MIL-53(Fe)-TDC.

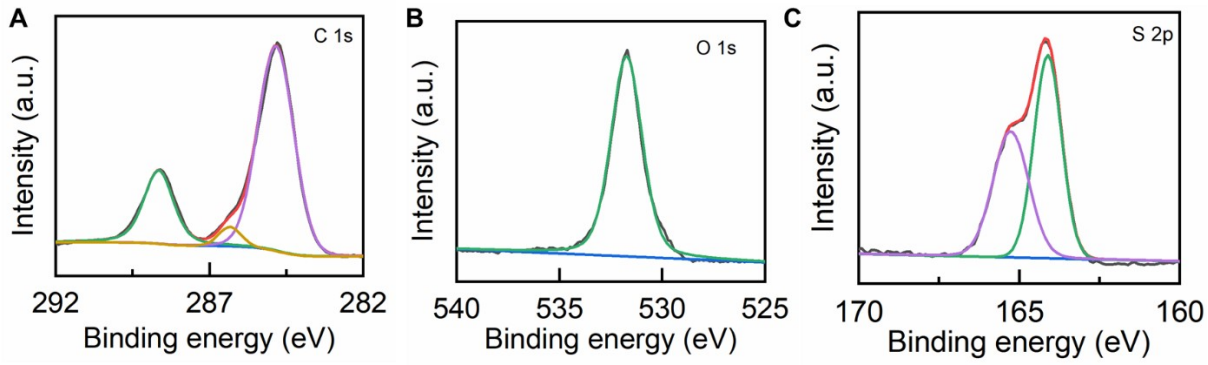

Fig. S2 High-resolution XPS spectra of C 1s, O 1s, and S 2p of MIL-53(Fe)-TDC.

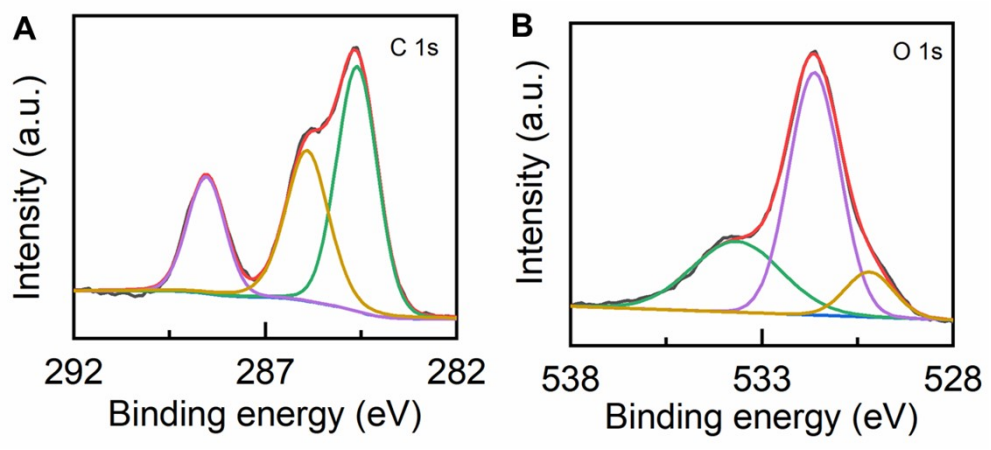

Fig. S3 High-resolution XPS spectra of C 1s, and O 1s of MIL-53(Fe)-FDC.

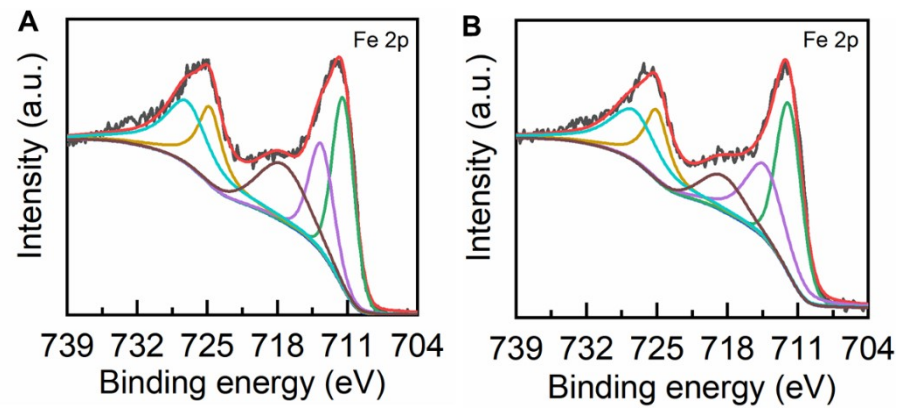

Fig. S4 High-resolution XPS spectra of Fe 2p for the MIL-53(Fe)-FDC (A) and MIL-53(Fe)-TDC (B).

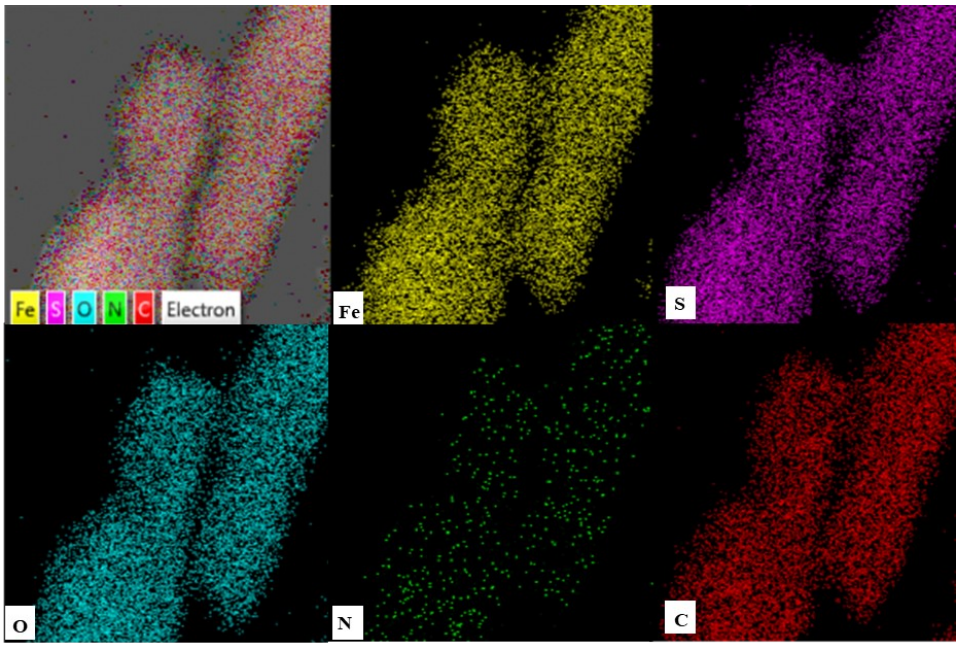

Fig. S5. Element mapping of the prepared MiL-53(Fe)-TDC.

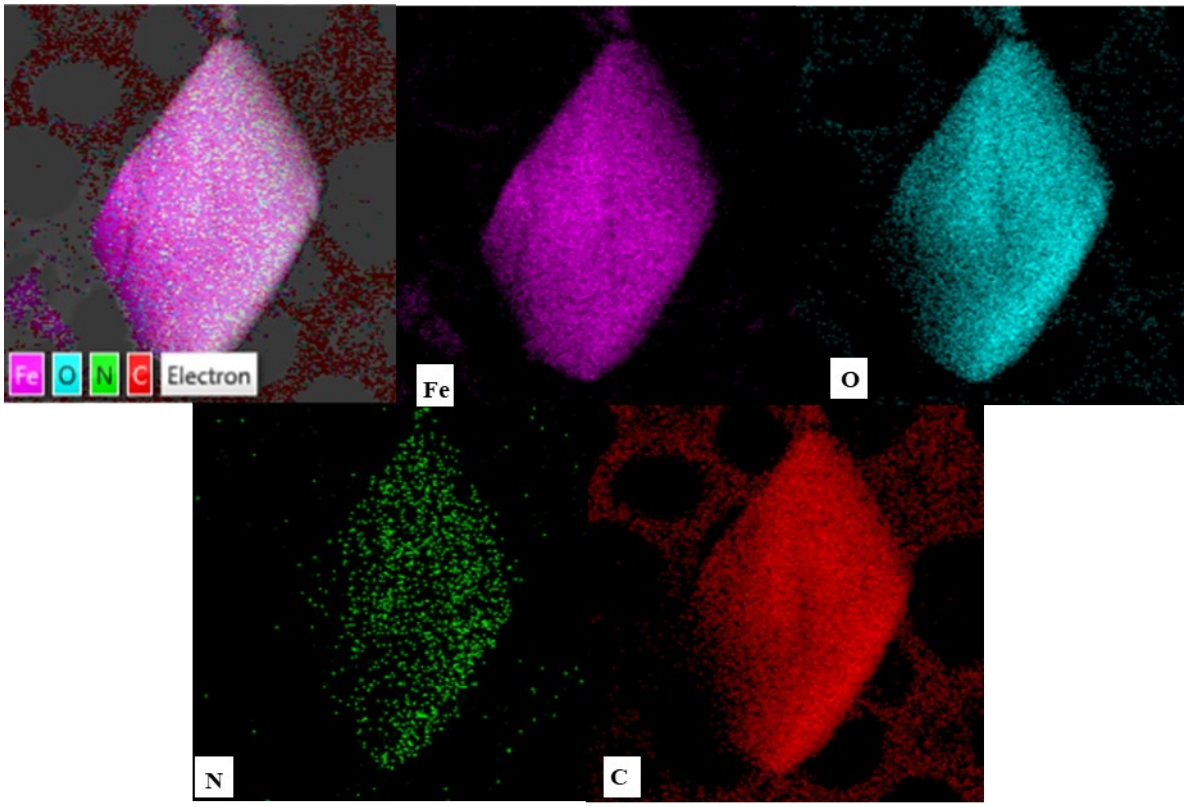

Fig. S6 Element mapping of the prepared MiL-53(Fe)-FDC.

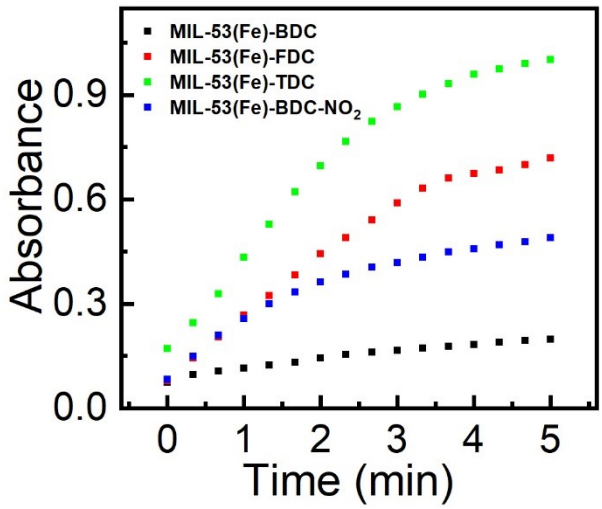

Fig. S7 Time-dependent absorbance variation of all the catalytic system.

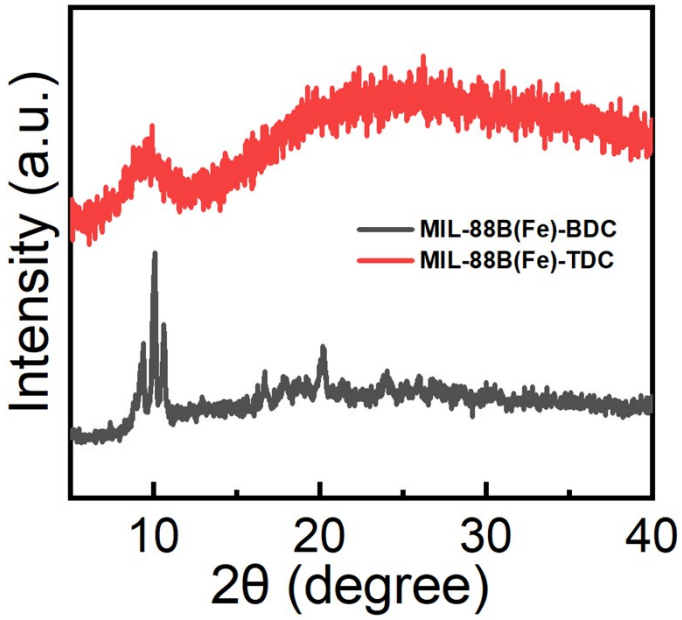

Fig. S8 PXRD patterns of MIL-88B(Fe)-L.

The diffraction peaks of MIL-88B(Fe)-BDC are nearly identical to those of the reported MIL-88B(Fe) with hexagonal symmetry (*Environ. Sci. Technol.* 2021, 55, 8341). In contrast, MIL-88B(Fe)-TDC exhibits low crystallinity, which can be attributed to its asymmetric structure.

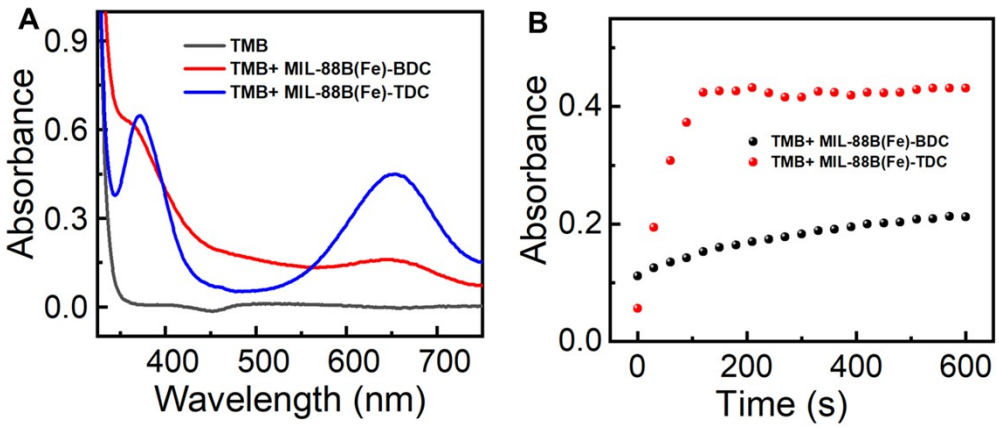

Fig. S9 (A) UV-vis spectra, and (B) Time-dependent absorbance variation of MIL-88B(Fe) nanozyme-based systems.

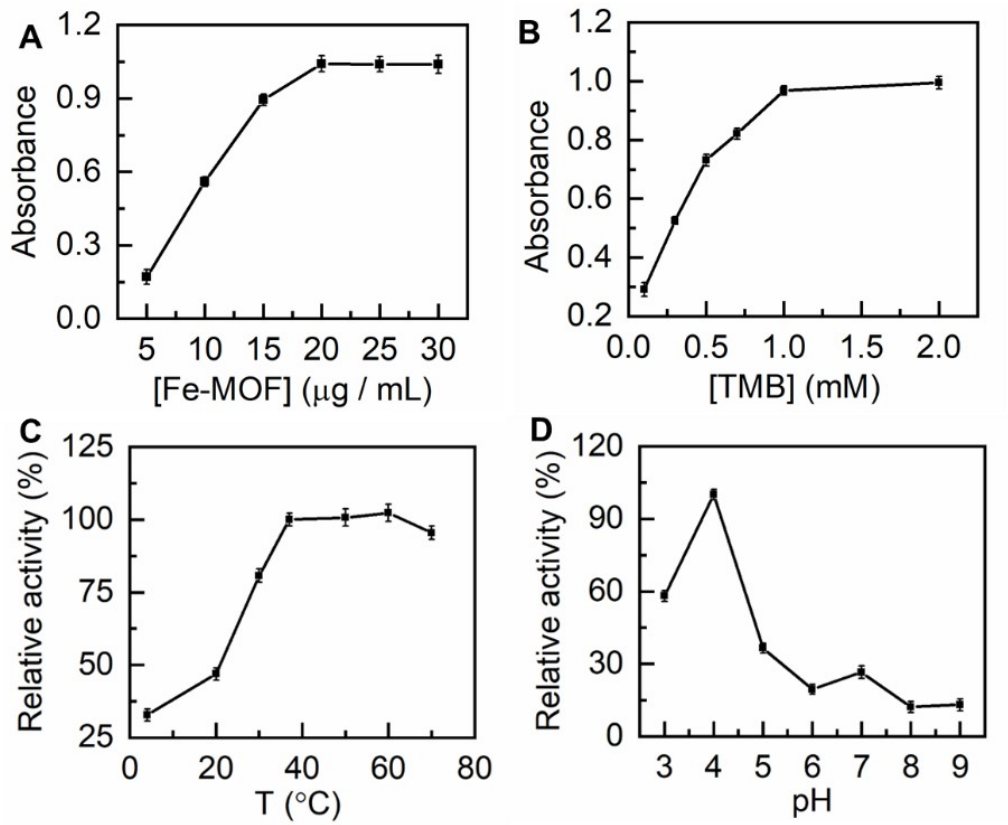

Fig. S10 The influence of nanozyme concentration (A), substrate concentration (B), temperature (C), and pH (D) on the catalytic activity of MIL-53(Fe)-TDC.

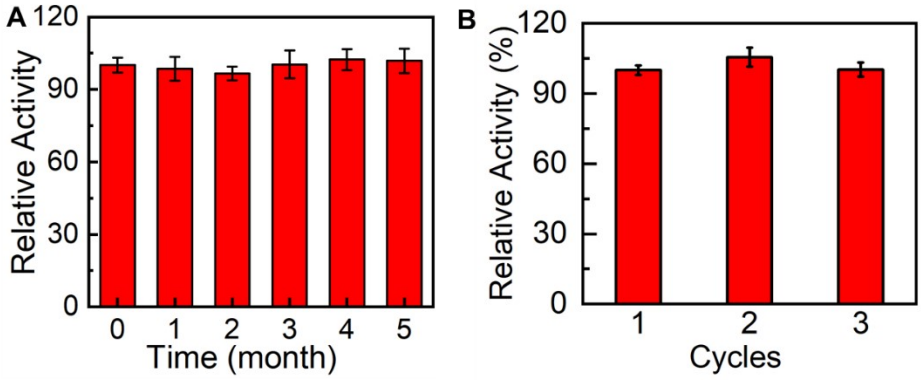

Fig. S11 The storage stability (A) and reusable performance (B) of MIL-53(Fe)-TDC

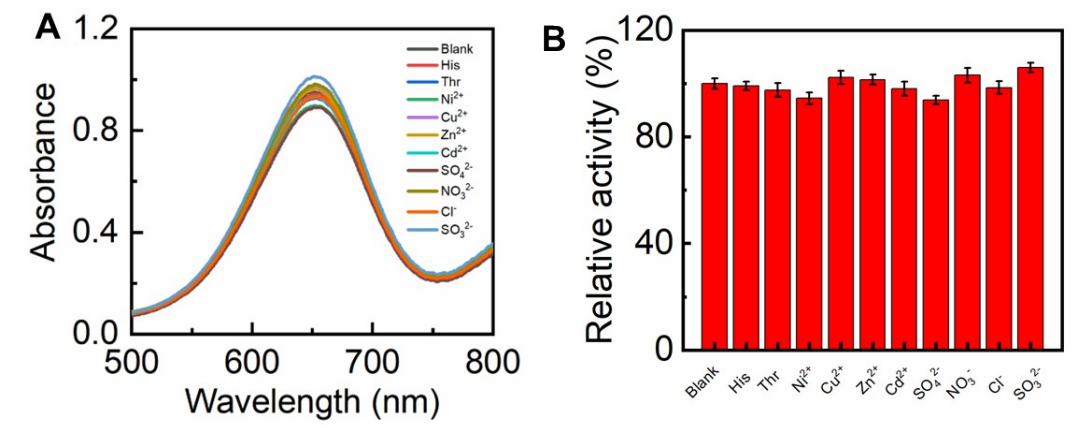

Fig. S12 The effect of interferers on the activity of MIL-53(Fe)-TDC.

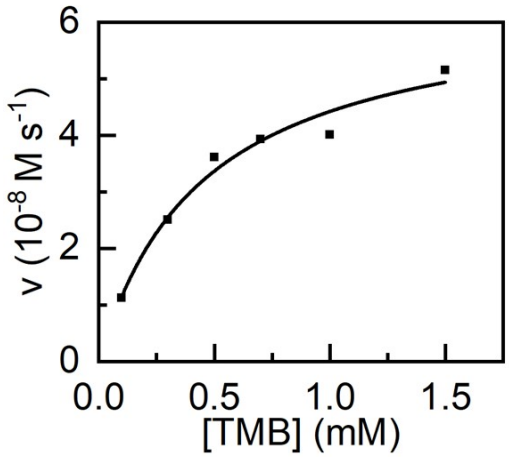

Fig. S13 the steady-state kinetic analysis of MIL-53(Fe)-FDC nanozyme.

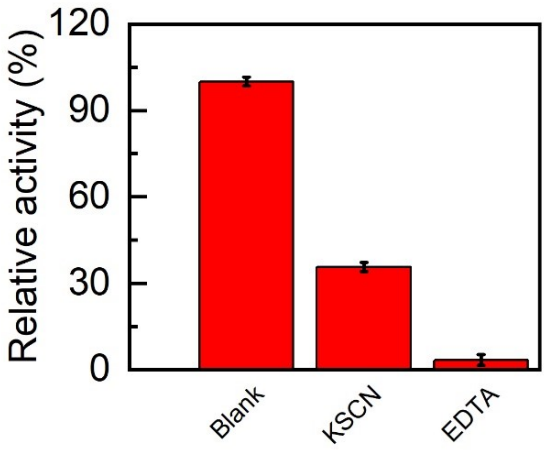

Fig. S14 Influence of chelating agent on the catalytic activity of MIL-53(Fe)-TDC.

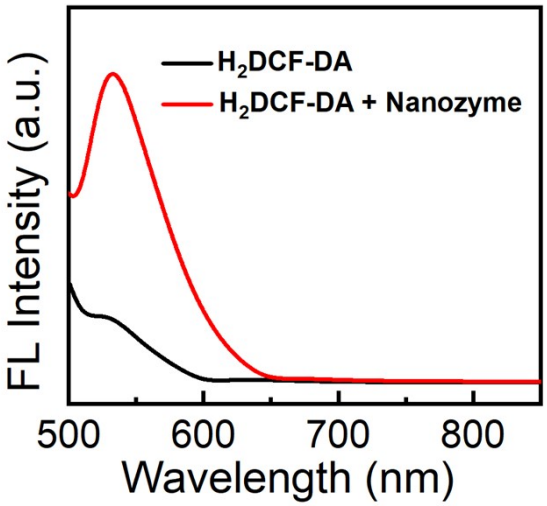

Fig. S15 Fluorescence intensity caused by reactive oxygen species.

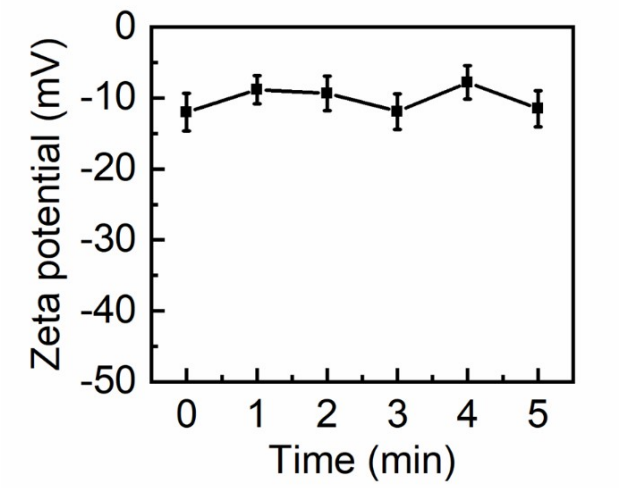

Fig. S16 zeta potential changes of catalytic system mediated by MIL-53(Fe)-TDC.

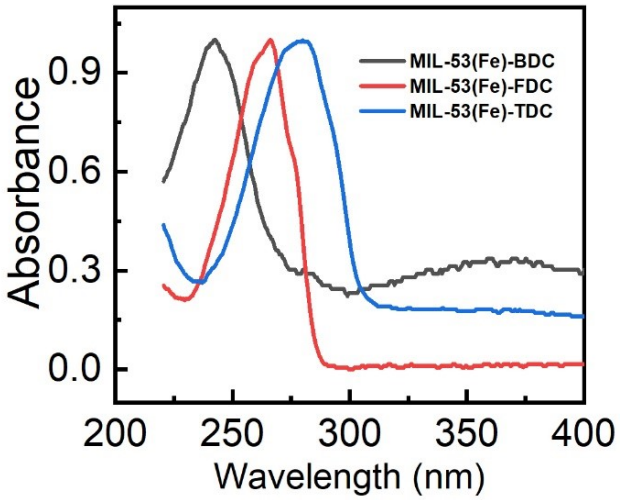

Fig. S17 Uv-Vis spectra of three MIL-53(Fe)- X nanozyme.